Cell Host & Microbe, Volume *20*

Supplemental Information

Dengue Virus Perturbs Mitochondrial Morphodynamics to Dampen Innate Immune Responses

Laurent Chatel-Chaix, Mirko Cortese, Inés Romero-Brey, Silke Bender, Christopher John Neufeldt, Wolfgang Fischl, Pietro Scaturro, Nicole Schieber, Yannick Schwab, Bernd Fischer, Alessia Ruggieri, and Ralf Bartenschlager

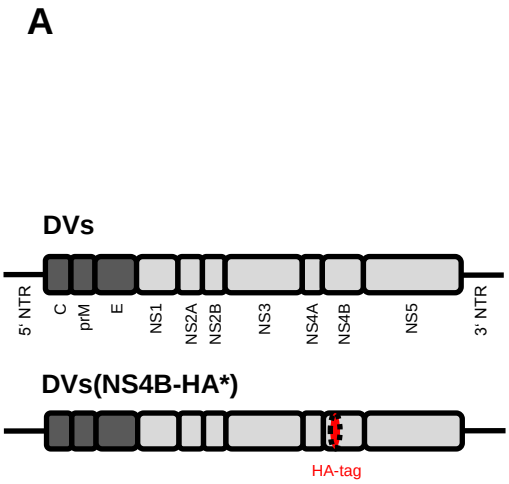

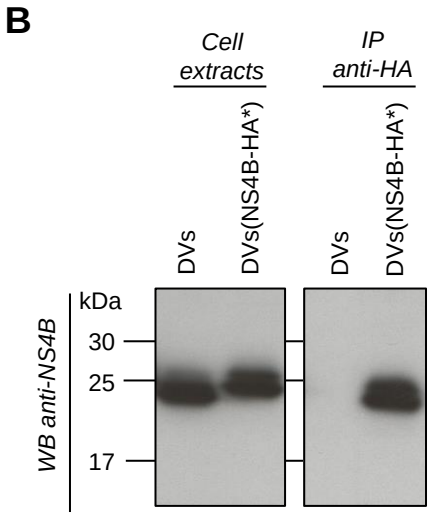

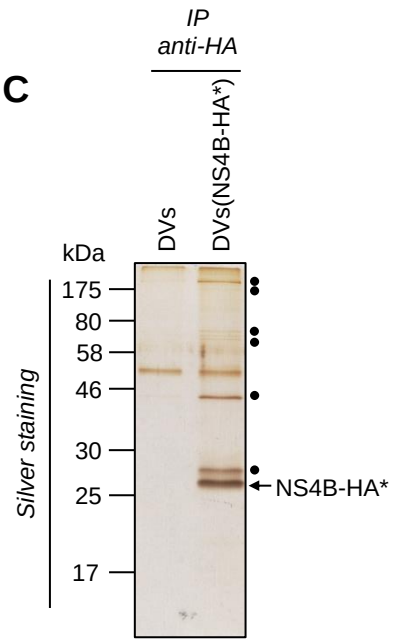

D

Name	ENSEMBL ID	Log2 Fold Enrichment	p-value
ATP5A1	ENSG00000152234	4.30	2.01E-07
ATP5B	ENSG00000110955	3.59	2.52E-07
CANX	ENSG00000127022	4.87	1.41E-05
GHITM	ENSG00000165678	Infinite	1.79E-04
SLC3A2	ENSG00000168003	Infinite	4.03E-04
ATP2A2	ENSG00000174437	Infinite	1.58E-03
ATP5O	ENSG00000241837	3.58	3.10E-03
HM13	ENSG00000101294	Infinite	4.40E-03
ATP5H	ENSG00000167863	Infinite	7.60E-03
VDAC2	ENSG00000165637	3.57	8.47E-03
ATP1A1	ENSG00000163399	Infinite	1.12E-02
APOB	ENSG00000084674	4.49	1.40E-02
IMMT	ENSG00000132305	Infinite	2.32E-02
MAOB	ENSG00000069535	Infinite	2.56E-02
HSPD1	ENSG00000144381	2.97	2.57E-02
ATP5C1	ENSG00000165629	3.67	3.21E-02
BAG2	ENSG00000112208	3.58	3.38E-02
ATP5F1	ENSG00000116459	3.38	4.52E-02
CHCHD3	ENSG00000106554	Infinite	4.79E-02

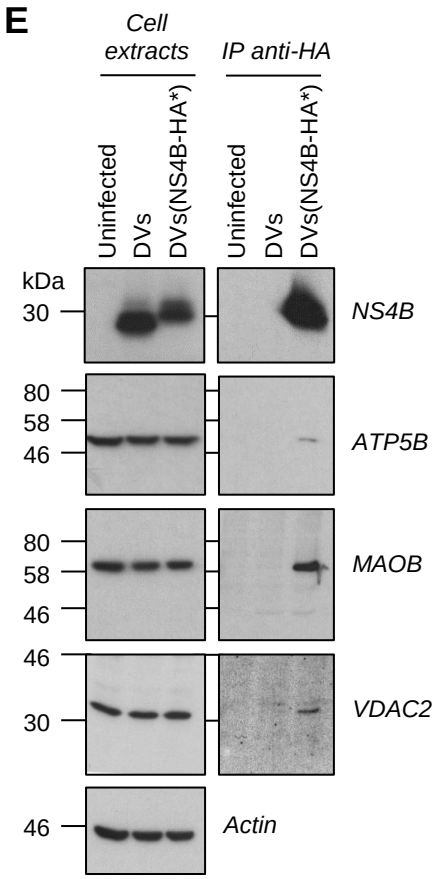

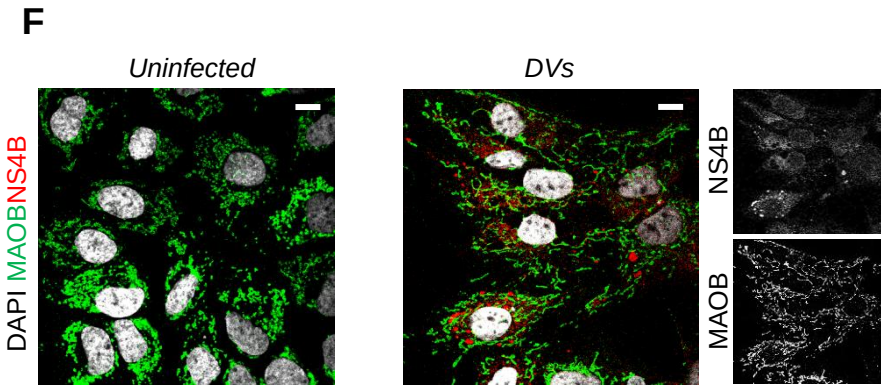

Figure S1

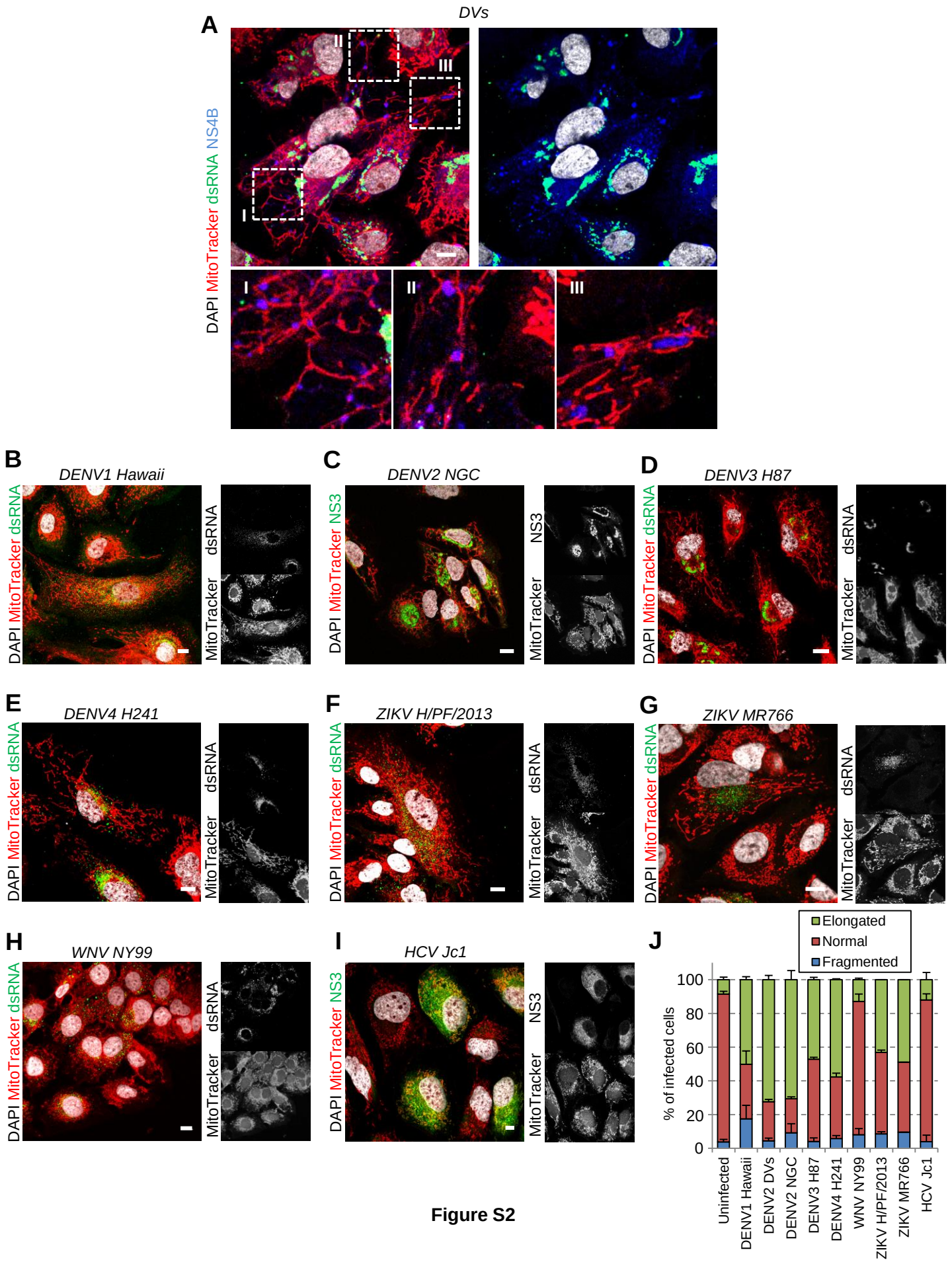
A
DVs
DAPI MitoTracker dsRNA NS4B
I
II
III
B
DENV1 Hawaii
C
DENV2 NGC
D
DENV3 H87
E
DENV4 H241
F
ZIKV H/PF/2013
G
ZIKV MR766
H
WNV NY99
I
HCV Jc1
DAPI MitoTracker dsRNA
MitoTracker dsRNA
DAPI MitoTracker NS3
MitoTracker NS3
J
Elongated
Normal
Fragmented
% of infected cells
0
20
40
60
80
100
Uninfected
DENV1 Hawaii
DENV2 DVs
DENV2 NGC
DENV3 H87
DENV4 H241
WNV NY99
ZIKV H/PF/2013
ZIKV MR766
HCV Jc1

Figure S2

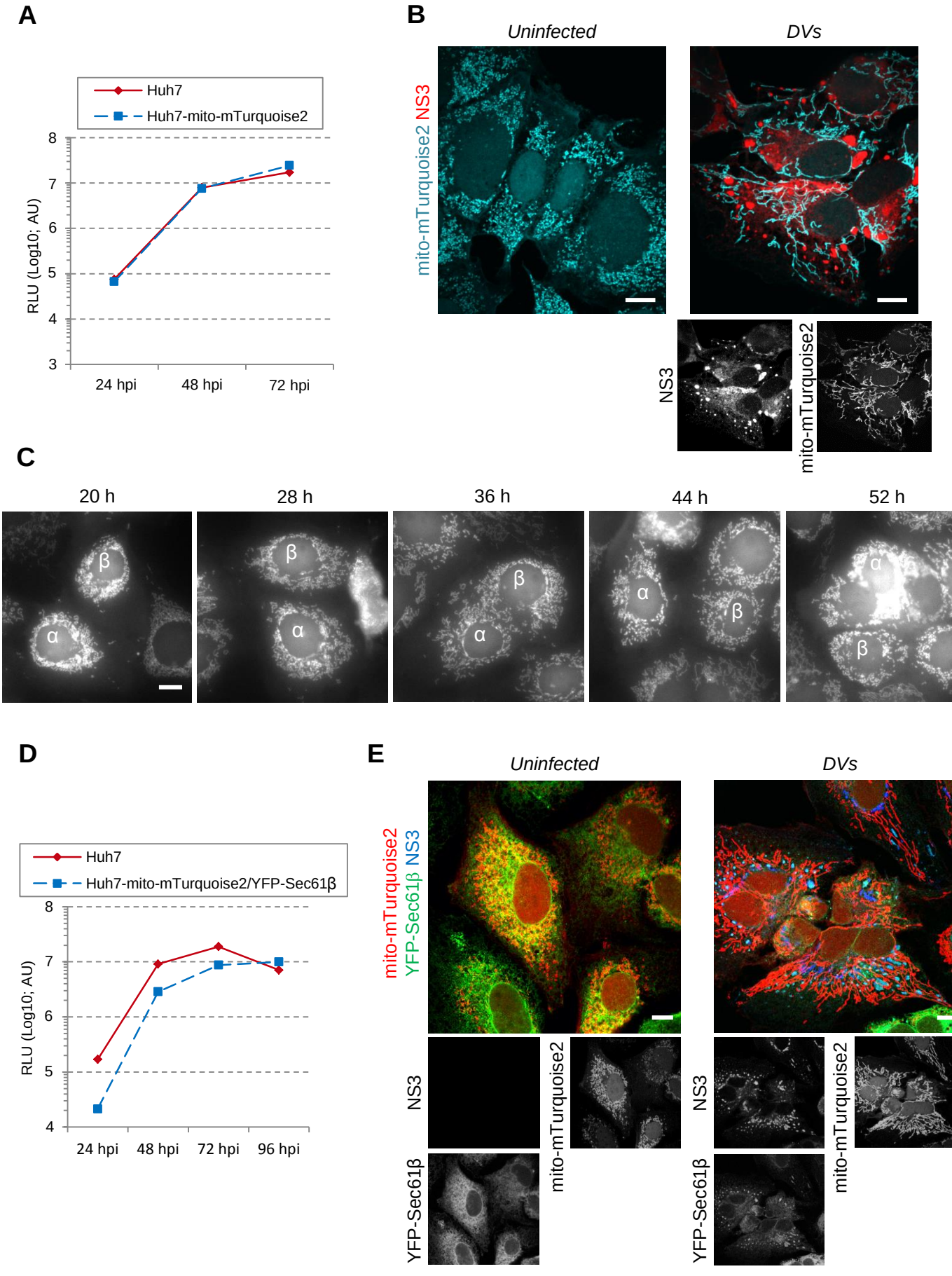
A
Huh7
Huh7-mito-mTurquoise2
RLU (Log10; AU)
8
7
6
5
4
3
24 hpi
48 hpi
72 hpi
B
Uninfected
DVs
mito-mTurquoise2 NS3
NS3
mito-mTurquoise2
C
20 h
28 h
36 h
44 h
52 h
Uninfected
β
α
D
Huh7
Huh7-mito-mTurquoise2/YFP-Sec61β
RLU (Log10; AU)
8
7
6
5
4
24 hpi
48 hpi
72 hpi
96 hpi
E
Uninfected
DVs
mito-mTurquoise2
YFP-Sec61β NS3
NS3
mito-mTurquoise2
YFP-Sec61β

Figure S3

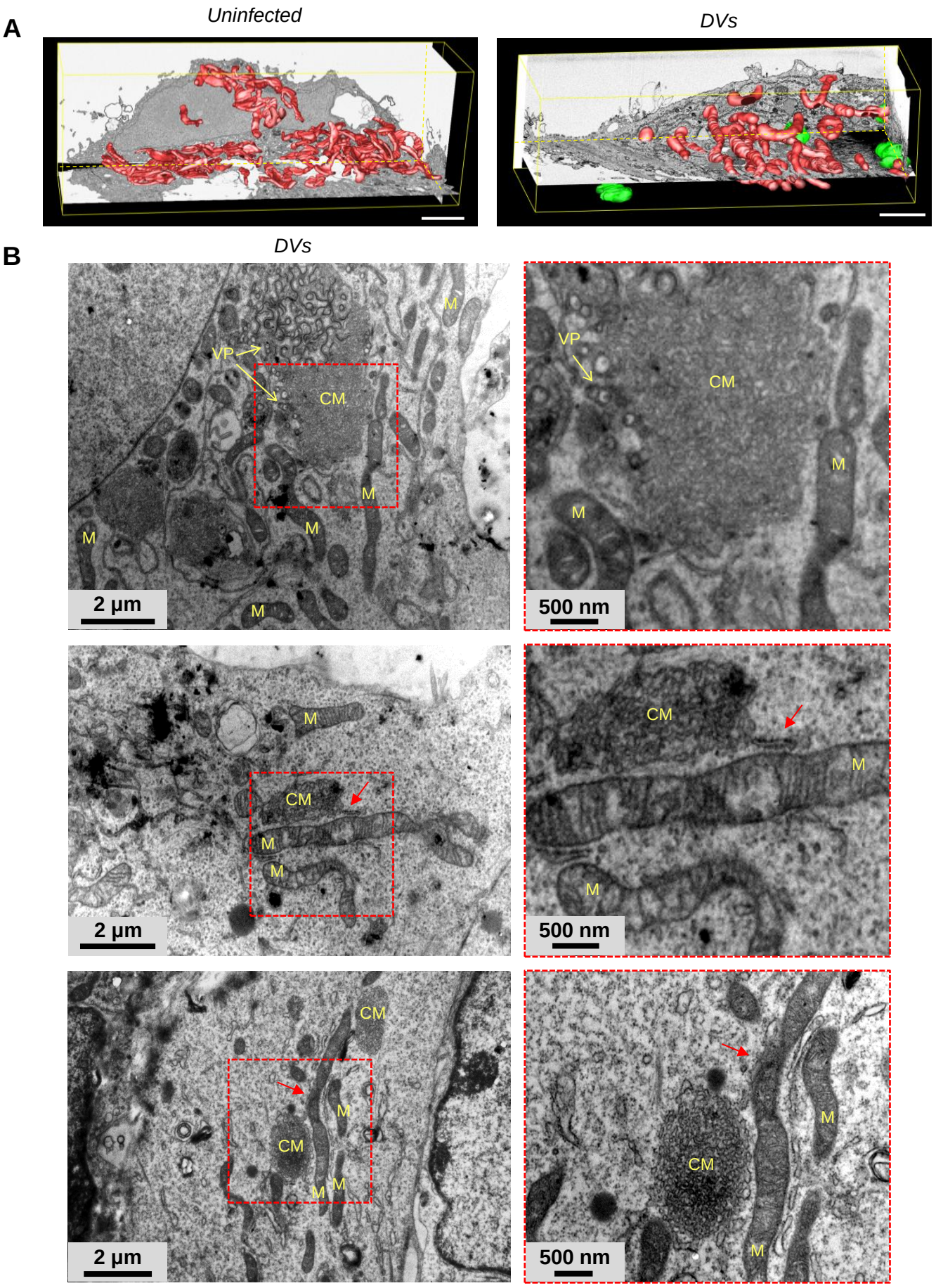

Figure S4

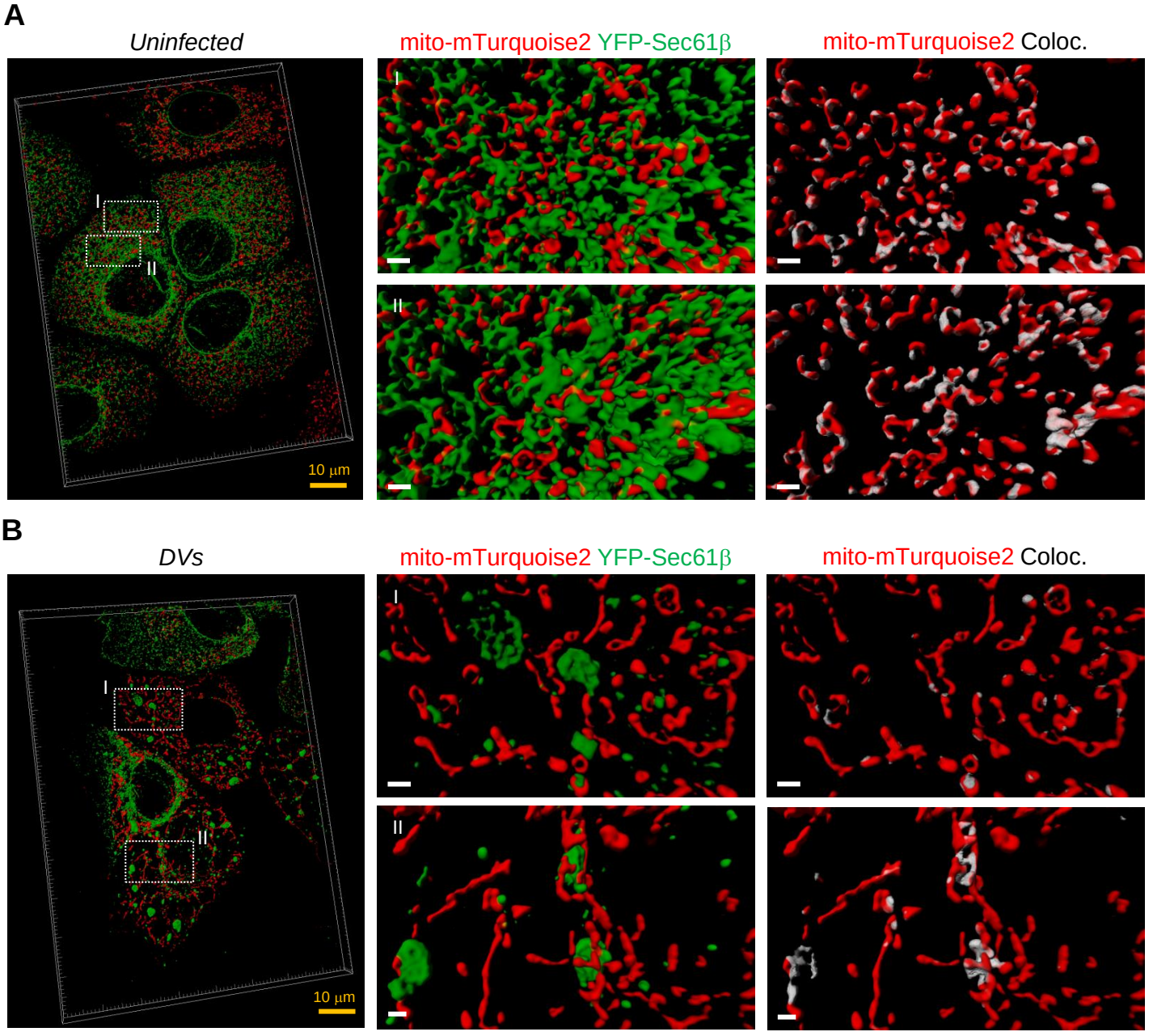
A
Uninfected
mito-mTurquoise2 YFP-Sec61β
mito-mTurquoise2 Coloc.
I
II
10 μm
B
DVs
mito-mTurquoise2 YFP-Sec61β
mito-mTurquoise2 Coloc.
I
II
10 μm

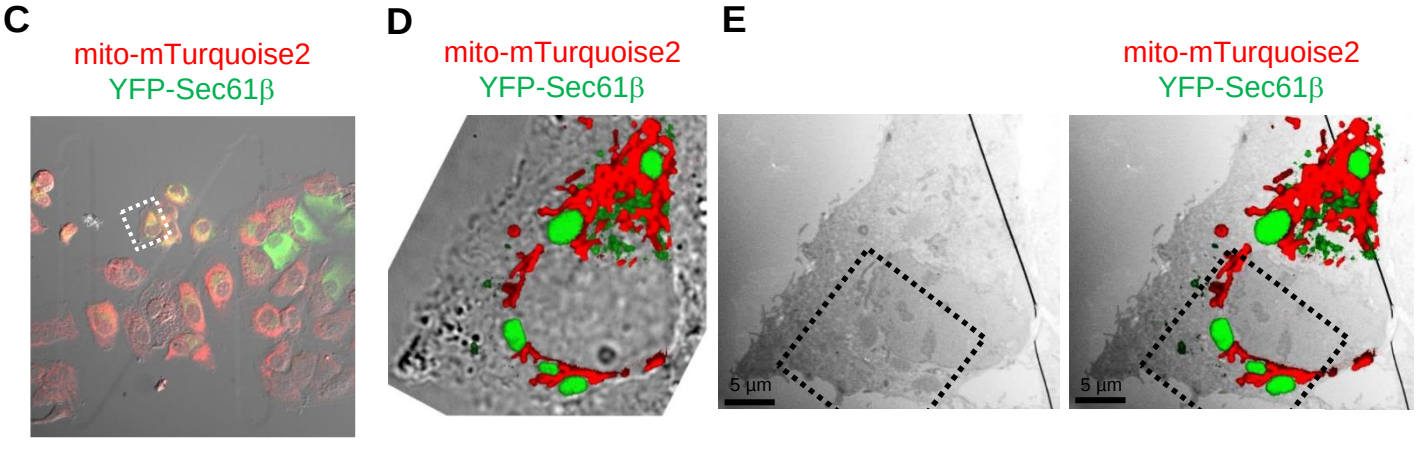
C
mito-mTurquoise2
YFP-Sec61β
D
mito-mTurquoise2
YFP-Sec61β
E
mito-mTurquoise2
YFP-Sec61β
5 μm
5 μm

Figure S5

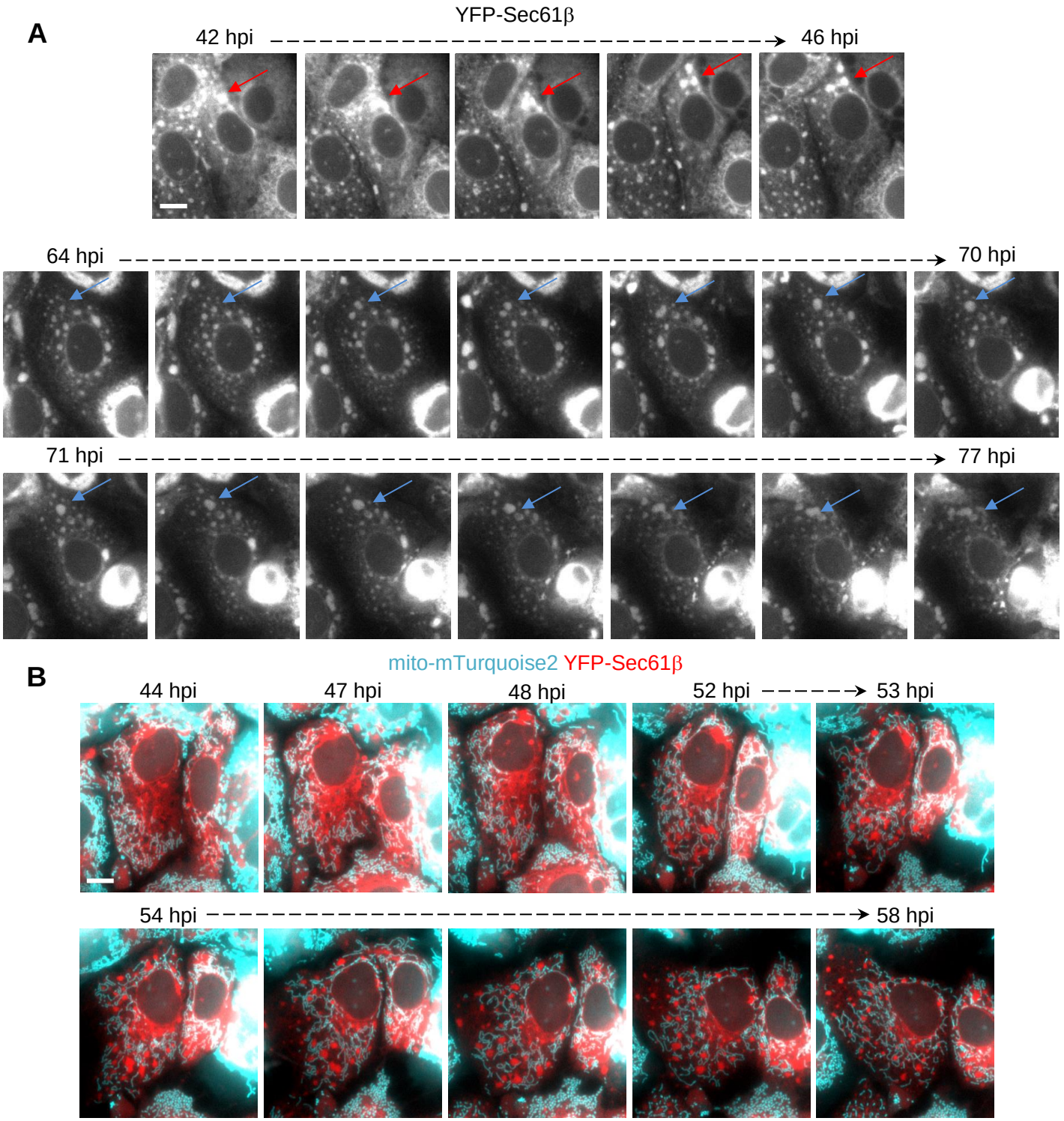
A
YFP-Sec61β
42 hpi
46 hpi
64 hpi
70 hpi
71 hpi
77 hpi
B
mito-mTurquoise2 YFP-Sec61β
44 hpi
47 hpi
48 hpi
52 hpi
53 hpi
54 hpi
58 hpi
C
ZIKV MR766
Fold (viral titers)
shNT
shDRP1
HCV JcR2A
Fold (RLU)
shNT
shDRP1

Figure S6

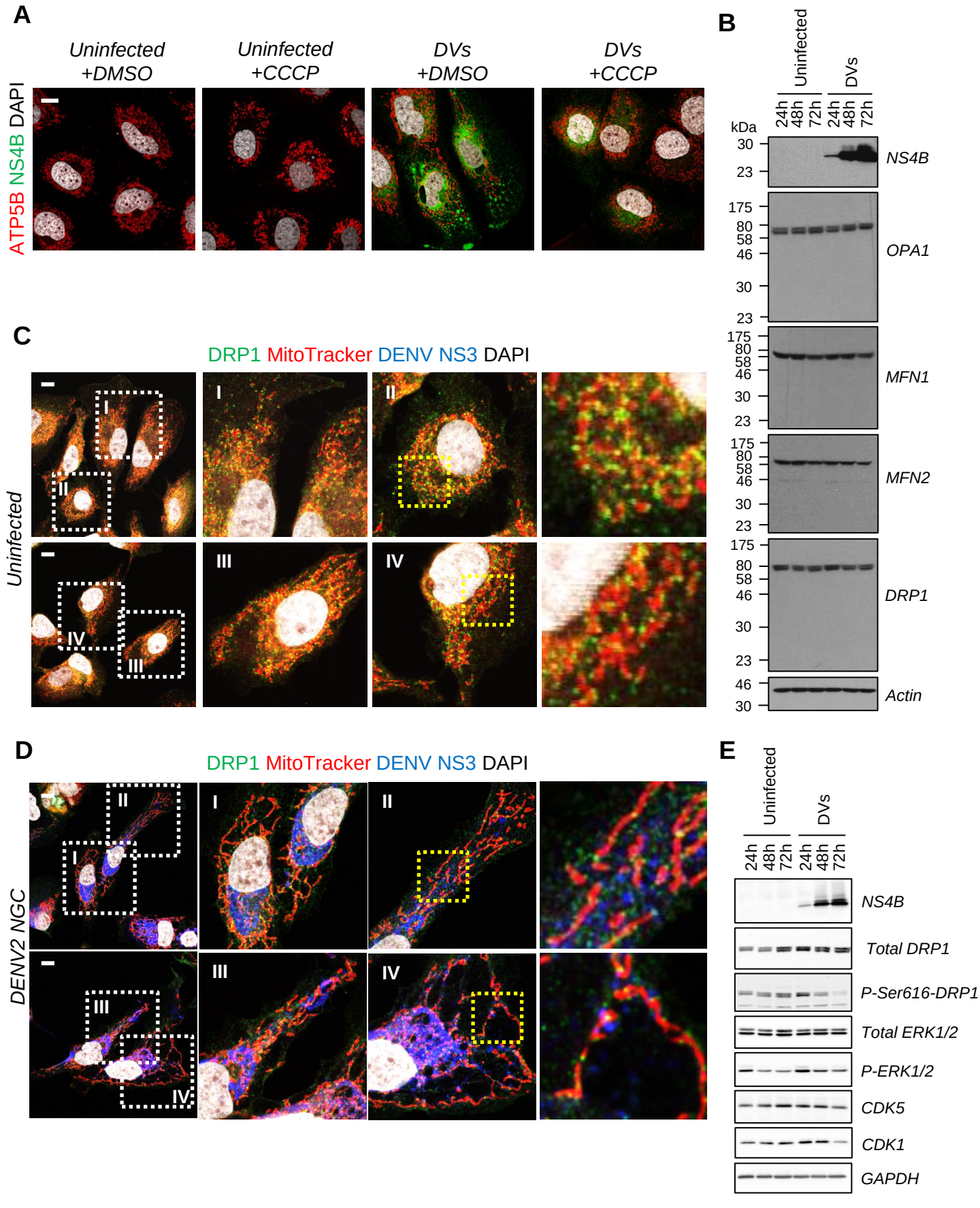
A
Uninfected +DMSO
Uninfected +CCCP
DVs +DMSO
DVs +CCCP
ATP5B NS4B DAPI
B
Uninfected
DVs
24h 48h 72h 24h 48h 72h
kDa
NS4B
OPA1
MFN1
MFN2
DRP1
Actin
C
DRP1 MitoTracker DENV NS3 DAPI
Uninfected
D
DRP1 MitoTracker DENV NS3 DAPI
DENV2 NGC
E
Uninfected
DVs
24h 48h 72h 24h 48h 72h
NS4B
Total DRP1
P-Ser616-DRP1
Total ERK1/2
P-ERK1/2
CDK5
CDK1
GAPDH

Figure S7

SUPPLEMENTAL INFORMATION

SUPPLEMENTAL FIGURE LEGENDS

Figure S1: Purification and identification of NS4B-associated host factors (related to Figure 1). (A) Schematic representation of the DENV2 16681s genomes expressing wt (DVs) or HA-tagged NS4B (DVs(NS4B-HA*)). Black lines represent 5' and 3' non translated regions (NTR). (B) Huh7 cells were infected with DVs or DVs(NS4B-HA*) virus stocks (MOI=5). Forty-eight hours later, cell extracts were prepared and subjected to immunoprecipitation using HA-specific antibodies. Cell extracts and immune complexes were analyzed by Western blotting with NS4B-specific antibodies. (C) Immunoprecipitates shown in (B) were analyzed using silver staining. • indicates proteins specifically co-purified with NS4B-HA* (indicated with the arrow). (D) Host proteins contained in NS4B-specific immunocomplexes were identified by GeLC-MS/MS using triplicate samples prepared as shown in (B) and (C). NS4B interactants were considered specific when enriched more than 8-fold ($p \leq 5x10^{-2}$) relative to the technical background that was determined with the DENV genome encoding the parental (non-tagged) NS4B (DVs). Mitochondrial proteins are written in red. Values were derived from three independent experiments. A complete list of the hits is given in Table S1. (E) Huh7 cells were infected with DVs or DVs(NS4B-HA*) virus stocks (MOI=1). Seventy-two hours later, cell extracts were prepared and subjected to HA-specific immunoprecipitation. Cell extracts and immune complexes were analyzed using Western blotting and the mitochondrial proteins ATP5B, MAOB and VDAC2 were validated as NS4B-interacting proteins. (F) Huh7 cells were infected with the DENV2 strain 16681 (DVs; MOI=1) or left uninfected. Three days later, cells were fixed, permeabilized and MAOB and NS4B were visualized by immunofluorescence using confocal microscopy. Scale bar: 10 µm.

Table S1: Mass spectrometry analysis of NS4B-HA*-containing protein complexes purified from DENV-infected cells (related to Figure 1). Host proteins contained in HA-specific immunocomplexes prepared from DVs- and DVs(NS4B-HA*)-infected cells were identified by GeLC–MS-MS using triplicate samples (EXP 1, EXP 2, EXP 3). For each identified protein, the ENSEMBL ID and the number of detected peptides in each replicate are shown. Enrichment factor (Log2 Fold Change) and significance for each identified protein were determined. NS4B-HA* interactants were considered specific when enriched more than 8-fold ($p \leq 5x10^{-2}$) relative to the technical background (DVs).

Movie S1: This movie shows fixed DENV2 DVs-infected Huh7 cells which were stained three days post-infection for mitochondria (red), NS3 (blue) and NS4B (green) and analyzed by confocal microscopy (related to Figure 1). Optical sections were acquired with a spinning disc confocal microscope and after deconvolution, Z-stacks were used for 3D reconstruction. The movie was generated with the Imaris 8 software package and shows the proximity of NS3/NS4B-containing punctae to DENV-induced elongated mitochondria.

Figure S2: All four DENV serotypes and ZIKV induce mitochondria elongation, but not WNV and HCV (related to Figure 1). Huh7 cells were infected at MOI=1-5 with (A) DVs, (B) DENV1 Hawaii, (C) DENV2 New Guinea C (NGC) strain, (D) DENV3 H87, (E) DENV4 H241, (F) ZIKV H/PF/2013, (G) ZIKV MR766, (H) WNV NY99 or (I) HCV Jc1. Thirty-six hours (NGC), 48 hours (WNV, ZIKV MR766, HCV) or 72 hours post-infection (all other samples), cells were incubated with MitoTracker, fixed, permeabilized and indicated proteins and dsRNA were visualized by immunofluorescence using confocal microscopy. Scale bar: 10 µm. (J) Quantification of the impact of virus infection on mitochondria morphology. The mitochondrial network of ~100 cells per condition and experiment (n=2-6) was examined and classified into three morphological categories (normal, fragmented, elongated) as described in supplemental experimental procedures.

Movie S2: Live cell imaging of Huh7-mito-mTurquoise2 cells left uninfected (left panel) or infected with DENV2 DVs (MOI=10; right panel) (related to Figure 1). Every hour, the signal in the Cyan channel was acquired. Time and scale bar are indicated in the movie. The movie shows time-dependent DENV-induced elongation of mitochondria until cell death because of cytopathic effects caused by DENV.

Movie S3: Live cell imaging of Huh7-mito-mTurquoise2 cells infected with DENV2 NGC (MOI=10) (related to Figure 1). The signal in the cyan channel was acquired every hour. Time post-infection and scale bar are indicated in the movie. The movie shows time-dependent DENV-induced elongation of mitochondria until cell death because of cytopathic effects caused by DENV.

Figure S3: Establishment of a stable Huh7 cell line suitable for visualization of mitochondria and ER in live cells (related to Figures 1 and 2). (A) Huh7 cells stably expressing the mTurquoise2 fluorophore fused with the

COX8 mitochondria-targeting signal (mito-mTurquoise2) were generated by lentiviral transduction. Cells were infected with the reporter virus DVs-R2A (MOI=0.1) and Renilla luciferase activity (RLU), used as a readout of DENV replication, was measured 24, 48 and 72 hours post-infection (hpi). Note that the reporter cells support DENV replication comparably to the parental non-transduced cells. AU: arbitrary units. (B) Huh7-mito-mTurquoise2 cells were infected with DVs (MOI=1). Three days post-infection, cells were fixed, permeabilized and NS3 was detected by immunofluorescence using confocal microscopy. Scale bar: 10 µm. (C) Live cell imaging frame captures of uninfected Huh7-mito-mTurquoise2 cells. Captures were made 20, 28, 36, 44 and 52 hours after a two-hour mock-infection and show a normal mitochondrial network. To facilitate tracking, two cells of interest are labeled with α and β. Scale bar: 10 µm. (D) Huh7 cells stably expressing mito-mTurquoise2 and YFP-Sec61β were generated by lentiviral transduction. Cells were infected with the DENV reporter virus DVs-R2A (MOI=0.1). Renilla luciferase activity (RLU) was measured 24, 48, 72 and 96 hours post-infection. Note that the simultaneous expression of the two fluorophore reporters has little effect on permissiveness to DENV. (E) Cells were infected with DVs (MOI=1). Three days later, cells were, fixed, permeabilized and NS3 was detected by immunofluorescence using confocal microscopy. Note the punctate staining pattern of NS3 that overlaps perfectly with YFP-Sec61β. Scale bar: 10 µm.

Movie S4: Three-dimensional reconstruction of the mitochondrial network in a DENV2 NGC-infected Huh7 cell (24 hours post infection; MOI=5) using focused ion beam/scanning electron microscopy (FIB/SEM) (related to Figure 2). Images of transversal sections of approximately 10 nm were acquired and used for 3D reconstruction. Reconstructed mitochondria are shown in red and DENV convoluted membranes in green. Note the elongated mitochondrial network with CMs in close proximity to mitochondria. Scale bar: 5 µm.

Figure S4: DENV-induced mitochondria elongation occurs in the vicinity of convoluted membranes (related to Figure 2). (A) Huh7 cells were infected with DVs (MOI=1) or left uninfected. Three days later, cells were processed for FIB/SEM as described in the Methods Online section. 3D reconstruction for mitochondria (red) and CM (green) was performed. Scale bar: 2 µm. (B) Sections of DVs-infected cells were analyzed with TEM. Magnification of regions of interest (red squares) are shown in the respective right panels to highlight that ER-mitochondria contact sites are partially disrupted in DENV-infected cells and that ER membranes are connected to CMs (red arrows). Yellow arrows indicate DENV-induced vesicle packets (VP). M: mitochondria.

Figure S5: DENV infection alters mitochondria-ER contacts (related to Figure 2). Huh7/mito-mTurquoise2/YFP-Sec61β cells were left uninfected (A) or infected with DVs (B). Three days later, cells were fixed and stained for NS3 (not shown). Optical sections were acquired with a spinning disc confocal microscope and after deconvolution, Z-stacks were used for 3D reconstruction and 3D colocalization analysis between mitochondria and YFP-Sec61β-signals (note that NS3-positive cells were considered infected). I-II: Magnifications of regions of interest show the mitochondria-ER contacts. White areas on reconstructed mitochondria (Coloc.) indicate regions of colocalization with YFP-Sec61β. White scale bar: 1 µm. (C-E) CLEM of a DVs-infected cell using YFP-Sec61β as a marker of NS3/NS4B-containing puncta. Mito-mTurquoise2/YFP-Sec61β-expressing cells were infected with DVs and processed for CLEM three days post-infection. The selected fixed cell was subjected to optical sectioning using a confocal microscope. (C) The 20x low magnification image of a combined phase contrast/fluorescence picture displays the cell of interest (white square) selected for high resolution analysis and shows the coordinate (Letter N) in the background. The mitochondria marker and YFP-Sec61β puncta are shown in red and green, respectively. (D) Combination of phase contrast and fluorescence images of the selected cell. (E) Superposition of a low magnification TEM image with the confocal microscopy Z-stack. Mitochondria were used to allocate the red fluorescent signal of a Z-stack to the proper ultrastructure and hence, for overall correlation. Higher resolution images of this cell are shown in Figure 3D-F.

Movie S5: Live cell imaging of uninfected Huh7/mito-mTurquoise2/YFP-Sec61β cells (related to Figure 3). Every hour, the signals in the Cyan and YFP channels were acquired. The movie shows the dynamics of the mitochondrial network. No accumulation of YFP-Sec61β punctae could be observed. Time and scale bar are indicated in the movie. Left: Combined imaging of both YFP-Sec61β and mito-Turquoise2. Right: Imaging of YFP-Sec61β only.

Movie S6: Live cell imaging of Huh7/mito-mTurquoise2/YFP-Sec61β cells infected with DVs (MOI=10) (related to Figure 3). Every hour, the signals in the Cyan and YFP channels were acquired. The movies show the dynamics of the mitochondrial network. The bottom movie highlights the continuous contacts between elongated mitochondria and CMs during infection. It also pinpoints the dynamic features of CMs undergoing merging and

division events (still images shown in Figure S6A). Time post-infection and scale bar are indicated in the movies. Left: Combined imaging of both YFP-Sec61β and mito-Turquoise2. Right: Imaging of YFP-Sec61β only. Still images of the top movie are shown in Figure S6B.

Figure S6: DENV-induced CMs are highly dynamic but remain in close proximity of mitochondria and ZIKV replication is influenced by DRP1 expression (related to Figures 3 and 5). Huh7/mito-mTurquoise2/YFP-Sec61β cells were infected with DVs (MOI=10) and analyzed by live-cell imaging. (A) Series of still images (from Movie S6, bottom) pinpointing the dynamic features of CMs. Within the same infected cell, division (red arrows) and merging (blue arrows) of CMs can be observed. Time points after infection are indicated in the top; images were taken every hour. (B) Time series of a cell of interest highlighting that CMs and mitochondria remain in close proximity throughout the observation period (from Movie S6, top). Scale bar: 10 µm. (C) Huh7 and Huh7.5 cells were transduced with shRNA-expressing lentiviruses and infected two days later with ZIKV MR677 (MOI=0.05) or HCV JcR2A (MOI=0.1), respectively. Two days post-infection, ZIKV titers and Renilla luciferase activity (RLU) reflecting HCV RNA replication were determined. Mean values of three (ZIKV) or two (HCV) independent experiments and corresponding SEM are shown. Related to Figure 5.

Figure S7: DENV infection does not affect the expression levels of the mitochondria fusion or fission factors while impeding DRP1 translocation to mitochondria (related to Figure 6). (A) Mitochondria elongation is important for the maintenance of DENV-induced CMs. Huh7 cells were infected with DVs at a MOI of 1 or left uninfected. Two days post-infection, cells were treated with 30 µM CCCP for 4 hours at 37^{o}C. After fixation and permeabilization, ATP5B and NS4B were detected by immunofluorescence using confocal microscopy. Scale bar: 10 µm. (B) Huh7 cells were infected with DVs (MOI=1) or left uninfected. At given time points after infection, cell extracts were prepared and analyzed by Western blotting using NS4B-, OPA1-, MFN1-, MFN2- and DRP1-specific antibodies. Actin detection was used to control for comparable protein amounts loaded onto each lane of the gel. (C-D) Huh7 cells were left uninfected (C) or infected with DENV2 NGC (MOI=5) (D). Thirty-six hours post-infection, cells were labeled with MitoTracker as well as DRP1- and NS4B-specific antibodies. Nuclear DNA was stained with DAPI. The white squares designate magnified regions of interest shown in the right of each panel. Further magnification of these images is indicated with yellow squares and shown on the right of each respective panel. Scale bar: 10 µm. (E) Huh7 cell extracts were generated exactly as in (B) and analyzed for the indicated proteins by Western blotting.

SUPPLEMENTAL EXPERIMENTAL PROCEDURES

Cell lines and virus strains

Huh7, 293T, VeroE6, HeLa and A549 cells were all cultured in Dulbecco's modified Eagle medium (DMEM, Life Technologies) containing 10% fetal bovine serum, 100 U/mL penicillin, 100 µg/mL streptomycin and 1% non-essential amino acids (complete DMEM). Stable Huh7 cell lines were cultured in medium containing either 2 ug/mL zeocin or 1ug/mL puromycin or both. DENV2 DVs virus stocks were prepared exactly as described earlier (Chatel-Chaix et al., 2015; Fischl and Bartenschlager, 2013) by electroporation of BHK-21 cells with in vitro transcribed DENV2 RNA and subsequent virus amplification in VeroE6 cells. DENV1 Hawaii, DENV2 New Guinea C (NGC), DENV3 H87, DENV4 H241, ZIKV H/PF/2013, ZIKV MR766 WNV NY99 virus stock were prepared by virus amplification in VeroE6 cells or insect C6/36 cells. All virus stocks were titrated using plaque assays.

Reagents

Carbonyl cyanide 3-chlorophenylhydrazone (CCCP) was obtained from Sigma-Aldrich. Production and characterization of rabbit anti-DENV NS3, anti-DENV NS4B, anti-DENV NS4A and anti-HCV NS3 were previously reported (Miller et al., 2006; Miller et al., 2007; Welsch et al., 2009; Koch and Bartenschlager, 1999). Mouse anti-DENV NS3 was obtained from GeneTex. All AlexaFluor-conjugated secondary antibodies and MitoTracker Red CMXRos were purchased from Life Technologies. Mouse anti-DRP1 and anti-OPA1 antibodies were purchased from BD Biosciences, mouse anti-MFN2, mouse anti-GAPDH and goat anti-MAOB antibodies from Santa Cruz Biotechnology, mouse anti-MFN1, rabbit anti-VDAC2, mouse anti-ATP5B and mouse anti-DENV NS1 antibodies from Abcam, mouse anti-β-actin and mouse anti-HA antibodies from Sigma-Aldrich, rabbit anti-phospho-Ser616-DRP1, rabbit anti-ERK1/2, rabbit anti-phospho-Thr201/Tyr204 ERK1/2, anti-phospho-Ser637-DRP1 and anti-COX IV antibodies from Cell Signaling, rabbit anti-calnexin from Stressgen, rabbit anti-FACL4

from BioCat, mouse anti-RIG-I from Alexis and mouse J2 anti-dsRNA antibodies from Scicons (English and Scientific Consulting Kft.).

DNA cloning

The plasmids containing the DENV2 16681s-based sequences of the full-length wild-type virus (pFK-DVs), the NS4B-HA-encoding virus, the Renilla luciferase (Rluc) reporter virus (pFK-DVs-R2A) and the sub-genomic reporter replicon (pFK-sgDVs-R2A) were described elsewhere (Chatel-Chaix et al., 2015; Fischl and Bartenschlager, 2013). The construction of pWPI-NS2B-3 and pTM-based expression plasmids encoding DENV HA-tagged NS4A, 2K-NS4B, NS4A-2K-NS4B and HCV JFH-1 NS3-5B polyprotein was previously reported (Chatel-Chaix et al., 2015; Reiss et al., 2011). Note that the 2K sequence in 2K-NS4B serves as signal peptide for NS4B membrane insertion; 2K is removed by the signalase generating mature NS4B. The construction of pWPI-mito-mTurquoise2 will be described elsewhere (A.R. and K. Rohr, in preparation). For lentiviral constructs expressing DENV2 proteins, sequences corresponding to NS4A, NS4B, 2K-NS4B and NS4A-2K-NS4B were amplified using PCR and pTM-based expression plasmids (Chatel-Chaix et al., 2015) as templates. PCR products were inserted into the BamHI/SpeI cassette of the pWPI plasmid. pENTR221-hDNM1L (a kind gift of Dr. Nathan R. Brady) was used to shuttle the human DRP1 coding sequence into pWPI-HA-puro using the Gateway recombination system (Life Technologies).

Co-immunoprecipitation assays and mass spectrometry

Co-immunoprecipitations were performed exactly as described previously (Chatel-Chaix et al., 2013). In brief, infected cells were lysed with dodecyl-β-maltoside-containing buffer and subjected to immunoprecipitation using anti-HA agarose beads (Sigma-Aldrich). For Western blot analysis, purified material was eluted with PBS containing 5% SDS and concentrated by acetone-mediated precipitation. For mass spectrometry-based identification of NS4B interactors, purified proteins were collected by three successive elutions using 100 µL of a 100 ng/µL HA peptide solution (Sigma-Aldrich). Pooled eluates were concentrated by acetone-mediated precipitation and submitted to GeLC-MS/MS (performed by the proteomics platform of the Institute of Microbiology, University of Greifswald, Germany). Protein composition of the resulting samples was determined using X!Tandem (version 2013.06.15). P-values from spectral counts were computed using the R/Bioconductor package DESeq and adjusted for multiple testing by the method of Benjamini-Hochberg (Benjamini and Hochberg, 1995). A cellular protein was considered as a NS4B interaction partner when it was significantly enriched more than 8-fold ($p \leq 5x10\text{-}2$) relative to the negative control which corresponded to cells infected with the non-tagged NS4B DENV that were processed in parallel.

Indirect immunofluorescence and confocal microscopy

Cells grown on coverslips were washed twice, fixed with PBS containing 4% paraformaldehyde for 20 minutes and permeabilized with 0.2% Triton-X100 in PBS. Coverslips were subjected to blocking with PBS containing 5% bovine serum albumin (BSA) and 10% goat serum. After washings, the cells were incubated with primary antibodies diluted in PBS/5% BSA for two hours. After three washes with PBS, cells were subjected to one-hour incubation with AlexaFluor 488-, 568-, or 647-conjugated secondary antibodies. Cells were washed three times with PBS for 15 minutes each and nuclei were stained with DAPI for 10 minutes. Coverslips were mounted on slides with FluoromountG (Southern Biotechnology Associates) and examined with a Leica SP2 laser scanning confocal microscope (Leica). For the quantification of mitochondria phenotypes, cells were observed with an inverted light microscope. The mitochondrial network of at least 100 cells per condition and experiment (2-6 independent replicates per virus) was examined and classified into three distinct categories (normal, fragmented and elongated morphology). A mitochondrial network was considered elongated when the elongation was observed at the whole cell level with at least 5 mitochondria longer than 15 µm (corresponding to the approximate diameter of a Huh7 cell nucleus). Mitochondria were classified as fragmented when $\geq$ 75 % of mitochondria appeared homogenously circular and with a diameter of ~1 µm in a dot-like pattern with no sign of elongation. Optical sections of 130 nm thickness were acquired with a Nikon TE2000-E inverted confocal microscope equipped with an Ultraview ERS spinning disc (PerkinElmer Life Sciences). Acquired pictures were subjected to deconvolution using Autoquant X3 software (Media Cybernetics). Three-dimensional reconstruction of cells and subsequent colocalization analyses were performed using the deconvolved Z-stacks and the Imaris 8 software package (Bitplane). For the analysis of NS4B-positive puncta (Figure 5J-K), cells were transduced with shRNA-expressing lentivirus and transfected three days later with plasmids encoding the DENV2 NS1-5 polyprotein. Fixed cells were labeled for immunofluorescence as described above. Optical sections of 300 nm thickness were acquired with a Leica SP8 inverted confocal

microscope using a 63x Plan-Apo N.A. 1.4 objective. Image analysis was performed using the Imaris 8 software package (Bitplane). Surface items were calculated on the NS4B signal using an absolute intensity thresholding of 30.8032. All surfaces smaller than 0.1 μm^2 were excluded. The average volume and the total number of surfaces for each cell were recorded.

Immuno-gold labelling

To fix the cells, one volume of 0.2 M PHEM buffer (120 mM PIPES, 50 mM HEPES, 4 mM $MgCl_2$, 20 mM EGTA, pH 6.9) containing 8% paraformaldehyde and 0.2% glutaraldehyde was added to the culture medium. Cells were incubated for 10 minutes at room temperature. After a second fixation for one hour with 0.1 M PHEM containing 4% paraformaldehyde and 0.1% glutaraldehyde, cell were stored in 0.1 M PHEM/4% paraformaldehyde at 4°C. Cells were washed for 10 minutes in 0.1 M PHEM/50 mM glycine and collected in 0.1 PHEM containing 1% gelatin. Cells were centrifuged, resuspended in pre-warmed 10% gelatin and spun down again. Cells were incubated on ice until the gelatin had solidified. Excess of cell-free gelatin was trimmed away and gelatin-embedded cells were cut into small cubes under a magnifying glass. The cubes were put into a 2.3 M sucrose solution and spun at 4°C overnight. Cell pellets were mounted on silver pins, flash-frozen and stored in liquid nitrogen. Samples were sectioned with a Reichert Ultracut S ultramicrotome using a Reichert FCS cryo-attachment and a Diatome diamond knife (Diatome). Cryosections were thawed and immunolabelled as previously described (Griffiths et al., 1983; Paul et al., 2013) using mouse anti-HA (Sigma-Aldrich) or immune-purified rabbit anti-NS3 primary antibodies (Welsch et al., 2009). Samples were examined using an EM-10 transmission electron microscope (Zeiss) with a built-in MegaView camera (Olympus).

Focused ion beam - scanning electron microscopy

Huh7 cells were infected with DENV (strains NGC and DVs; MOI 5) and fixed with 2.5% glutaraldehyde (Electron Microscopy Sciences) and 0.1% malachite green oxalate (Sigma) in 0.1 M PHEM buffer. Cells were washed with 0.1 M PHEM buffer and stored at 4°C until further processing in a PELCO BioWave Pro microwave processor (Ted Pella, Inc.). For post-fixation samples were incubated with 1% osmium tetroxide (Electron Microscopy Sciences) and 0.8% potassium hexacyanoferrate(III) ($K_3Fe(CN)_6$; Merck) in 0.1 M PHEM. Cells were rinsed with 0.1 M PHEM, incubated with 0.5% uranyl acetate in water, rinsed with water, dehydrated with increasing concentrations of ethanol (25, 50, 75, 90 and 100%) and embedded with a graded series of Epon (Serva). Epon-infiltrated cells were incubated at 55°C to polymerize the resin. The part of the resin block containing the cells was mounted onto a SEM stub (Agar Scientific) using carbon sticker (Plano, GmBH, Wetzlar) and surrounded with silver paint (Pelco Colloidal Silver, Ted Pella Inc.) with the cells pointing upwards, perpendicular to the electron column. Samples were sputter-coated with gold (Quorum, GaLa Instrumente GmbH) for 120 sec at 30 mA. Images were recorded with a dual beam Auriga 60 FIB-SEM microscope (ZEISS), equipped with a gallium ion source for focused ion beam milling and a field emission gun scanning electron microscope. The specimen stage was tilted to 54° and exposed to the focused ion beam in a way that the stage of the plane was parallel to the ion beam. Prior to milling and imaging, the sample surface was coated with platinum (~1 µm) using the gas injection system to cover the region of interest (on average 50 μm^2). All sample preparation and acquisition settings were performed using the Atlas3D software package (FIBICS Inc.). A cross sectional cut was introduced in two stages. First, a cut was made at high beam current (typically 16 nA) and at an accelerating voltage of 30 kV to create a trench that enabled viewing of the cross-section. In the second step, the ion beam was scanned using a current of 2 nA to polish and smooth the surface. SEM imaging was done using the ESB (back-scattered electron) detector at 1.5 kV, with a pixel size of 10 nm in x/y. For slice-and-view image series, a z-step of ~10 nm was chosen to remove the material from the specimen surface with the focused ion beam in order to obtain isotropic datasets. All acquired images were combined as a stack using the FIJI (ImageJ) software package and aligned using the TrakEM2 plugin. Finally, the contrast of all images was inverted to obtain the contrast of conventional TEM images. Organelles of interest were rendered using the IMOD software package (version 4.7).

Transfection

Electroporation of Huh7 cells with in vitro transcripts of DENV genomes was performed exactly as described earlier (Chatel-Chaix et al., 2015). Huh7 cells stably expressing T7 RNA polymerase and in some experiments in addition the NS2B-NS3 protease (Chatel-Chaix et al., 2015) were grown on glass coverslips and transfected with pTM-based plasmids using TransIT-LT1 (Mirus) according to the manufacturer's instructions. Culture medium was changed 4 hours later. Cells were processed for indirect immunofluorescence 24 hours post-transfection.

Lentivirus production and transduction of cells

Stable knock-down of selected genes and overexpression of DENV proteins was achieved through transduction with lentiviruses encoding distinct shRNAs and proteins, respectively. For production of lentivirus stocks, sub-confluent 293T cells were transfected with packaging plasmids pCMV-Gag-Pol and pMD2-VSV-G (kind gifts from Dr. Didier Trono) and shRNA-encoding pLKO-puro plasmids obtained from Sigma-Aldrich or pWPI-based plasmids using 25 kD linear polyethylenimine (Polysciences Inc.) as previously described (Chatel-Chaix et al., 2013). Two days post-transfection, lentivirus-containing medium was collected and filtered. Lentiviruses were titrated by transducing HeLa cells and subsequent treatment with 1 ug/ml puromycin. Five days later, cells were fixed and stained with 1% crystal violet/10% ethanol for 15-30 minutes. Stained cells were rinsed with water, colonies were counted and titers calculated taking into account inoculum dilution. For all experiments, transductions were typically performed using a MOI of 5 for Huh7 or 3 for A549 cells in the presence of 4 µg/mL polybrene. The pLKO plasmids TRCN0000001097 and TRCN0000082686 (Sigma Aldrich) were used to knockdown the expression of DRP1 and MFN2, respectively. The non-targeting shRNA-encoding plasmid SHC002 (Sigma-Aldrich) was used as negative control and reference. Cell viability of transduced cells was evaluated using the CellTiter-Glo Luminescent Cell Viability Assay kit (Promega) measuring ATP amounts according to the manufacturer's instructions. Luminescence was measured with a Mithras LB940 plate reader (Berthold Technologies). The same transduction approach was used to produce Huh7 cells expressing YFP-tagged Sec61β and mitochondria-targeted mTurquoise2. Cells expressing the latter were selected with 2 µg/ml zeocin and then, transduced with YFP-Sec61β-encoding lentiviruses. After double selection with 1 µg/mL puromycin and 2 µg/mL zeocin, cells were used for CLEM. For live cell imaging analyses, cells expressing high levels of these markers were sorted using flow cytometry prior to expansion.

Virus titration and replication measurement

Titers of infectious virus were determined using plaque assays as previously described (Metz et al., 2015). In brief, VeroE6 cells were infected with virus preparations that had been serially diluted in complete DMEM. Approximately two hours post-infection, the inoculum was removed and cells were cultured at 37˚C with serum-free MEM (Life Technologies) containing 1.5% carboxymethylcellulose. Several days post-infection (depending on the virus strain), cells were fixed by 2 hours incubation with formaldehyde (5% final concentration). After extensive washes with water, cells were stained with 1% crystal violet/10% ethanol for 15-30 minutes. Stained cells were rinsed with water, plaques were counted and titers of infectious virus were calculated. RNA replication of DENV2 (DVs-R2A) reporter virus was determined by measuring the activity of virus-encoded Renilla luciferase (Rluc) exactly as previously described (Chatel-Chaix et al., 2015; Fischl and Bartenschlager, 2013). After lysis of the cells, coelenterazine (1.43 µM final concentration) was added and luminescence was measured using a Lumat LB9507 luminometer (Berthold Technologies).

Real-time RT-PCR

Total RNA was purified from cells using the Nucleospin RNA isolation kit (Macherey-Nagel) according to the instructions of the manufacturer. cDNAs were generated using the High Capacity cDNA Reverse Transcription kit (Applied Biosystems) and used for real-time PCR with the iTaq Universal SYBR Green kit (Bio-Rad) and the following specific primer pairs: GAAGGTGAAGGTCGGAGTC and GAAGATGGTGATGGGATTTC for GAPDH; AGCACTGTGTTGGCGTACAG and GACTTCGAGCAAGAGATGG for β-actin; GAAGCAGGCAATCACAGAAA and TGAAACCGACCATAGTGGAA for ISG56; CAGCTCCAAGAAAGGACGAAC and GGCAGTGTAACTCTTCTGCAT for IFN-β; GCAGGTTCAAATCTCTGTCACC and AAGACAGGAGAGCTGCAACTC for IFN-λ1 (Bender et al., 2015). Amplification reactions and measurements were carried out using a C1000 Touch Thermal cycler (CFX96 realtime system; Bio-Rad).

Generation of RIG-I knockout cell lines using CRISPR/Cas9 technology

Knock-out of RIG-I in Huh7 cells was achieved by using the CRISPR/Cas9 system as previously described (Shalem et al., 2014). In brief, two different single-guide RNAs (sgRNAs) were designed targeting the second exon of the coding region of RIG-I with the help of the open source tool (Heigwer et al., 2014) and inserted into the lentiviral vector lentiCRISPR v2 (Addgene #52961) also encoding the Cas9 nuclease. The following sgRNAs were used: 5'

CTGTTGGAGCTCCAGGAGGA 3' (KO-1) and 5' TGGAGCTCCAGGAGGAAGGC 3' (KO-2). Lentiviruses were produced as described above and used to transduce Huh7 cells. Cell populations were selected with 1 ug/mL puromycin and tested for RIG-I expression using Western blotting.

Sub-cellular fractionation and MAM isolation

The procedure used to isolate mitochondria-associated membranes (MAMs) was previously described (Horner et al., 2011; Neufeldt et al., 2013; Neufeldt et al., 2016; Wieckowski et al., 2009). Briefly, cells were lysed using a Balch homogenizer (Isobiotec) followed be removal of nuclei and cellular debris by low speed centrifugation. Mitochondria and associated membranes were then pelleted from the supernatant and MAMs were separated from the mitochondria by centrifugation through a percoll gradient. Total protein amount in each fraction was determined using Bradford assays. Protein contents were evaluated by SDS-PAGE and Western blotting. FACL4 and calnexin were used as marker enriched in the MAM fraction and α-tubulin as a cytosolic marker.

Statistical analysis

Standard deviation (SD) (on representative experiments) was calculated using at least three technical replicates. Standard error to the mean (SEM) was determined based on at least three independent experimental replicates (except if stated otherwise). Statistical significance was evaluated by determining p-values using the Student's t-Test (two-tailed distribution). A result was considered significant when the p-value was below 0.05.

SUPPLEMENTAL REFERENCES

Bender,S., Reuter,A., Eberle,F., Einhorn,E., Binder,M., and Bartenschlager,R. (2015). Activation of Type I and III Interferon Response by Mitochondrial and Peroxisomal MAVS and Inhibition by Hepatitis C Virus. PLoS. Pathog. *11*, e1005264.

Benjamini,Y. and Hochberg,Y. (1995). Controlling the false discovery rate: a practical and powerful approach to multiple testing. Journal of the Royal Statistical Society. Series B *57*, 289-300.

Chatel-Chaix,L., Germain,M.A., Motorina,A., Bonneil,E., Thibault,P., Baril,M., and Lamarre,D. (2013). A host YB-1 ribonucleoprotein complex is hijacked by hepatitis C virus for the control of NS3-dependent particle production. J. Virol. *87*, 11704-11720.

Fischl,W. and Bartenschlager,R. (2013). High-throughput screening using dengue virus reporter genomes. Methods Mol. Biol. *1030*, 205-219.

Griffiths,G., Simons,K., Warren,G., and Tokuyasu,K.T. (1983). Immunoelectron microscopy using thin, frozen sections: application to studies of the intracellular transport of Semliki Forest virus spike glycoproteins. Methods Enzymol. *96*, 466-485.

Heigwer,F., Kerr,G., and Boutros,M. (2014). E-CRISP: fast CRISPR target site identification. Nat. Methods *11*, 122-123.

Koch,J.O. and Bartenschlager,R. (1999). Modulation of hepatitis C virus NS5A hyperphosphorylation by nonstructural proteins NS3, NS4A, and NS4B. J. Virol. *73*, 7138-7146.

Metz,P., Chiramel,A., Chatel-Chaix,L., Alvisi,G., Bankhead,P., Mora-Rodriguez,R., Long,G., Hamacher-Brady,A., Brady,N.R., and Bartenschlager,R. (2015). Dengue Virus Inhibition of Autophagic Flux and Dependency of Viral Replication on Proteasomal Degradation of the Autophagy Receptor p62. J. Virol. *89*, 8026-8041.

Miller,S., Sparacio,S., and Bartenschlager,R. (2006). Subcellular localization and membrane topology of the Dengue virus type 2 Non-structural protein 4B. J. Biol. Chem. *281*, 8854-8863.

Neufeldt,C.J., Joyce,M.A., Levin,A., Steenbergen,R.H., Pang,D., Shields,J., Tyrrell,D.L., and Wozniak,R.W. (2013). Hepatitis C virus-induced cytoplasmic organelles use the nuclear transport machinery to establish an environment conducive to virus replication. PLoS. Pathog. *9*, e1003744.

Neufeldt,C.J., Joyce,M.A., Van,B.N., Levin,A., Kirkegaard,K., Gale,M., Jr., Tyrrell,D.L., and Wozniak,R.W. (2016). The Hepatitis C Virus-Induced Membranous Web and Associated Nuclear Transport Machinery Limit Access of Pattern Recognition Receptors to Viral Replication Sites. PLoS. Pathog. *12*, e1005428.

Paul,D., Hoppe,S., Saher,G., Krijnse-Locker,J., and Bartenschlager,R. (2013). Morphological and biochemical characterization of the membranous hepatitis C virus replication compartment. J. Virol. *87*, 10612-10627.

Reiss,S., Rebhan,I., Backes,P., Romero-Brey,I., Erfle,H., Matula,P., Kaderali,L., Poenisch,M., Blankenburg,H., Hiet,M.S., Longerich,T., Diehl,S., Ramirez,F., Balla,T., Rohr,K., Kaul,A., Buhler,S., Pepperkok,R., Lengauer,T., Albrecht,M., Eils,R., Schirmacher,P., Lohmann,V., and Bartenschlager,R. (2011). Recruitment and activation of a lipid kinase by hepatitis C virus NS5A is essential for integrity of the membranous replication compartment. Cell Host. Microbe *9*, 32-45.

Shalem,O., Sanjana,N.E., Hartenian,E., Shi,X., Scott,D.A., Mikkelsen,T.S., Heckl,D., Ebert,B.L., Root,D.E., Doench,J.G., and Zhang,F. (2014). Genome-scale CRISPR-Cas9 knockout screening in human cells. Science *343*, 84-87.

Wieckowski,M.R., Giorgi,C., Lebiedzinska,M., Duszynski,J., and Pinton,P. (2009). Isolation of mitochondria-associated membranes and mitochondria from animal tissues and cells. Nat. Protoc. *4*, 1582-1590.